



Efficiency enhancement in dye-sensitized solar cells by interfacial modification of conducting glass/mesoporous TiO₂ using a novel ZnO compact blocking film

Yumin Liu^a, Xiaohua Sun^a, Qidong Tai^a, Hao Hu^a, Bolei Chen^a, Niu Huang^a, Bobby Sebo^a, Xing-zhong Zhao^{a,b,*}

^a Department of Physics and Technology, Wuhan University, Wuhan 430072, People's Republic of China

^b Key Laboratory of Artificial Micro/Nano Structures of Ministry of Education, Wuhan University, Wuhan 430072, People's Republic of China

ARTICLE INFO

Article history:

Received 26 April 2010

Received in revised form 30 June 2010

Accepted 13 July 2010

Available online 17 July 2010

Keywords:

Zinc oxide compact film

Energy barrier

Electron density

Dye-sensitized solar cells

Electrochemical properties

ABSTRACT

A novel and thin ZnO compact blocking film is employed at the interface of fluorine-doped tin oxide (FTO) substrate and mesoporous TiO₂, and its influence on dye-sensitized solar cells (DSSCs) is investigated. The ZnO film prepared by spin-coating method on FTO is characterized by energy-dispersive X-ray spectroscopy (EDX), scanning electron microscopy (SEM), and UV–vis spectrophotometer. The ZnO film is firstly employed as an energy barrier between FTO and mesoporous TiO₂ film in DSSCs, which improves open-circuit photovoltage (V_{oc}) and fill factor (FF) with compensation of J_{sc} decrease, finally increasing energy conversion efficiency from 5.85% to 6.70%. Electrochemical impedance spectra (EIS) analysis and open-circuit voltage decay (OCVD) technique reveal that the existence of the energy barrier not only resulted in the effect of suppressing back electrons transfer from FTO to electrolyte but also blocking the electrons injection from the conductive band of TiO₂ to FTO. The former effect effectively reduces the recombination which occurs in the region of FTO substrate, and the latter leads to remarkable increment of electron density in the TiO₂, thus resulting in enhanced V_{oc} and FF. These results suggest that the methodology of introducing the semiconductor with a more negative conduction band edge than TiO₂ as the compact blocking film in DSSCs may be feasible.

Crown Copyright © 2010 Published by Elsevier B.V. All rights reserved.

1. Introduction

Dye-sensitized solar cells (DSSCs) based on nanocrystalline TiO₂ have attracted extensive attentions in academic research and industrial applications since O' Regan et al. reported their breakthrough discovery in 1991 [1], and may offer an alternative to conventional semiconductor-based solar cells due to their low cost and high efficiencies. DSSC is typically composed of a mesoporous nanocrystalline TiO₂ film covered by a monolayer of dye molecules, electrolyte, and counterelectrode. Recently, a range of fabrication procedures have been applied to modify their interfaces to improve the performance of the device. Such as electrode surface modification of TiO₂ through introducing Nb₂O₅ [2], ZnO [3,4], MgO [5,6], Al₂O₃ [7,8], and so on, mainly focuses on the decrease of the interfacial charge recombination by forming an energy barrier between the TiO₂ electrodes and the electrolyte. In addition, many efforts have been made to investigate the interface of electrode/dye [9,10] and dye/electrolyte [11] to optimize the interfacial dynamics. On the other hand, a few groups have also studied the interface of conducting glass/TiO₂ mainly to investigate its effect on the per-

formance of DSSCs by employing a compact film [12–14]. However, research on such important interface is not intense as compared to modification of the others.

Zhu et al. [15] reported that recombination occurs predominantly in the region of fluorine-doped tin oxide (FTO) substrate rather than homogeneously across the depth of the TiO₂ film based on the results from Intensity-Modulated Infrared Spectroscopy (IMIS) analysis. So it is essential to introduce an efficient compact blocking layer to the FTO glass surface to decrease the charge recombination between electrons emanating from the FTO substrate and I₃⁻ ions present in the electrolyte. In the past decade, a majority of the researches on the interface of FTO/TiO₂ employed TiO₂ as the compact film [16–18], and they found that the influence of TiO₂ compact layer is extremely relevant for the determination of DSSCs parameters. It has been reported by Xia et al. [19,20] that an effective Nb₂O₅ blocking layer by sputtering method to create a potential barrier between the FTO substrate and TiO₂, which improved open-circuit photovoltage and fill factor, and kept good short-circuit photocurrent density (J_{sc}) by controlling the thickness of Nb₂O₅ layer. Recently, Nb doped-TiO₂ (NTO) thin film deposited on FTO substrate to form a compact film for DSSCs by pulsed laser deposition (PLD), which achieved an obvious effect has been reported [21,22]. Nevertheless, Nb₂O₅ and NTO are expensive compact materials, and the methods of sputtering or PLD may not be the

* Corresponding author. Tel.: +86 27 87642784; fax: +86 27 87642569.

E-mail address: xzzhao@whu.edu.cn (X.-z. Zhao).

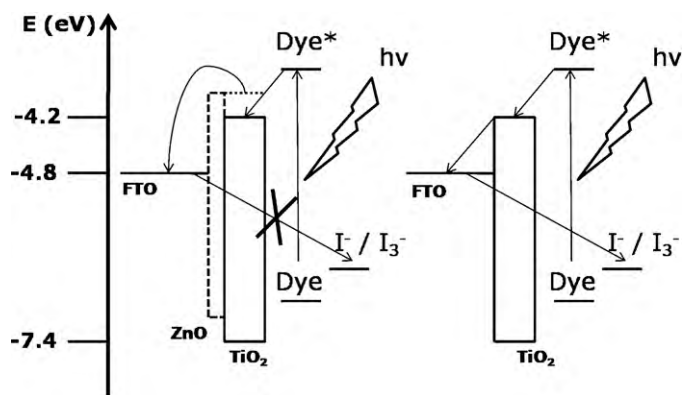


Fig. 1. Schematic view of the electron transfer with and without ZnO layer.

best choice for industrialization due to the high cost of manufacturing process. On the other hand, it is revelatory for us to suppose that a methodology of introducing an energy barrier at FTO/TiO₂ interface rather than the surface of TiO₂ electrode may be feasible.

ZnO is one of the promising semi-conducting materials in the domain of solar energy conversion due to its stability against photocorrosion and photochemical properties. Several researches have employed ZnO to reduce the recombination at electrode/electrolyte interface as having a more negative conduction band edge than TiO₂ [3,4,23]. However, it has never been applied as a compact film at the interface of FTO/TiO₂, probably due to its foreseeable blocking effect for the electrons injection from TiO₂ to FTO. It has also been reported by Horiuchi et al. [24] that ZnO can be dissolved to some extent by forming an aggregate with N3 sensitizer, and this formation of N3-Zn²⁺ will lead to an inefficient electron injection. However, the effect of this aggregate plays little role in the present case, since the ZnO layer was compact and almost covered by mesoporous TiO₂ film which resulted in a small portion of ZnO exposed to the sensitizer, and the electrons was mainly injected into the conductive band of ZnO from mesoporous TiO₂ film rather than the sensitizer. So this aggregation will not influence considerably the electron transfer in the photoelectron conversion process.

In this paper, we report a low-cost effective ZnO compact blocking film at FTO/TiO₂ interface by a facile spin-coating method, which mainly plays the role of creating an energy barrier between FTO substrate and TiO₂ film. This potential barrier will result in the following two effects to charge transport at the interface of FTO and TiO₂: (a) suppressing back electrons transfer from FTO to electrolyte; and (b) blocking the electrons injection from the conductive band of TiO₂ to FTO which would further affect the electron density in TiO₂. The latter effect has seldom been reported probably because the blocking effect of electrons injection to FTO is considered to be useless. In this study, however, we make use of this blocking effect to increase the electron density in TiO₂, and thus the rise of Fermi level, which will improve V_{oc} remarkably. The schematic view of electron transfer with and without ZnO layer is shown in Fig. 1. We report here the details of the fabrication and the characterization of ZnO film. Furthermore, we discuss its effect to the photoelectron conversion process by current-voltage characteristics, open-circuit voltage decay (OCVD) technique and electrochemical impedance spectroscopy (EIS) analysis of the devices, which support our foregoing supposition.

2. Experimental

2.1. Materials

Poly (ethylene glycol) (PEG, MW = 20,000), Triton-X100, Zinc acetate, diethanolamine (DEA), HNO₃, CH₃COOH, and propy-

lene carbonate (PC) were obtained from Sinopharm Chemical Reagent Corporation (China). Lithium iodide (LiI, 99%), 4-tert-butylpyridine (TBP) and titanium tetraisopropoxide (98%) were purchased from Acros. Iodine (I₂, 99.8%) was obtained from Beijing Yili chemicals (China). The Ru dye, *cis*-di(thiocyanato)-bis(2,2'-bipyridyl-4,4'-dicarboxylate) ruthenium(II) (N719), were purchased from Solaronix (Switzerland). All the reagents used were of analytical purity. Fluorine-doped SnO₂ conductive glass (FTO, sheet resistance 10–15 Ω sq⁻¹, Asahi Glass, Japan) were used as the substrate for spin-coating the ZnO compact blocking layer and the deposition of mesoporous nanocrystalline TiO₂ film.

2.2. Preparation and characterization of ZnO compact blocking film.

ZnO film was prepared with the method reported previously [25]. In short, Zinc acetate was added into 50 ml of absolute ethanol under stirring (50 °C). When the solution changed into a white emulsion, an amount of DEA was added into the emulsion, the molar ratio of DEA/Zinc acetate being 1:1. The emulsion then became clear immediately. After stirring for about 10 min, the content became a steady homogeneous sol without any precipitation. To investigate the effects of ZnO layer on the performance of DSSCs, spin-coating method was applied to coat the zinc acetate sol at different concentration (0.1–0.5 M) on the clean FTO substrates with the same rotate speed and time. The coating films were dried in air for 30 min, and then sintered at 500 °C for an hour to form ZnO compact blocking layer.

Energy-dispersive X-ray spectroscopy (EDX, GENESIS 7000) was used to determine the chemical species of the composite substrates. The thickness of ZnO film was measured with a TalyForm S4C-3D profilometer (UK). The surface morphology of ZnO compact blocking layer was observed by scanning electron microscopy (SEM, Sirion FEG, USA). UV-vis adsorption spectra were recorded on a UV-vis-NIR spectrophotometer (Cary 5000, Varian).

2.3. Device fabrication

TiO₂ colloid which was synthesized by hydrolysis of titanium tetraisopropoxide according to the reported procedure [26] was used to prepare mesoporous nanocrystalline TiO₂ film by a doctor-blading technique. The edges of the conducting glass were covered with adhesive tapes as the frame. To make the TiO₂ films with the same thickness, the concentration of TiO₂ colloid and the layer numbers of tapes were same for each sample. The TiO₂ colloids was spread on both bare FTO and FTO/ZnO substrates, followed by sintering at 500 °C for 30 min. The thickness of the film was 10 μm, as measured with a TalyForm S4C-3D profilometer (UK). The mesoporous TiO₂ electrode was preheated at 120 °C for 20 min, and then immersed into the solution of *cis*-di(thiocyanato)-bis(2,2'-bipyridyl-4,4'-dicarboxylate) ruthenium(II) with a concentration of 500 μM in the mixture of acetonitrile and *tert*-butyl alcohol (volume ratio: 1/1) at 60 °C for 12 h. Then the electrodes were washed with acetonitrile to remove the accumulated dye molecules on the surface of nanocrystalline TiO₂ to ensure that the film was covered with a monolayer of dye molecules. A sandwich-type DSSC configuration was fabricated by assembling the dye-loaded mesoporous TiO₂ with platinum plate counter electrode. The assembled cell was then clipped together as an open cell. An electrolyte composed of 0.1 M 1-propyl-3-methylimidazolium iodide (PMII), 0.05 M LiI, 0.1 M GNCS, 0.03 M I₂, 0.5 M 4-*tert*-butylpridine (TBP) in mixed solvent of acetonitrile and propylene carbonate (PC) (volume ratio: 1/1) was injected into the open cell from the edges, and then the cell was tested immediately.

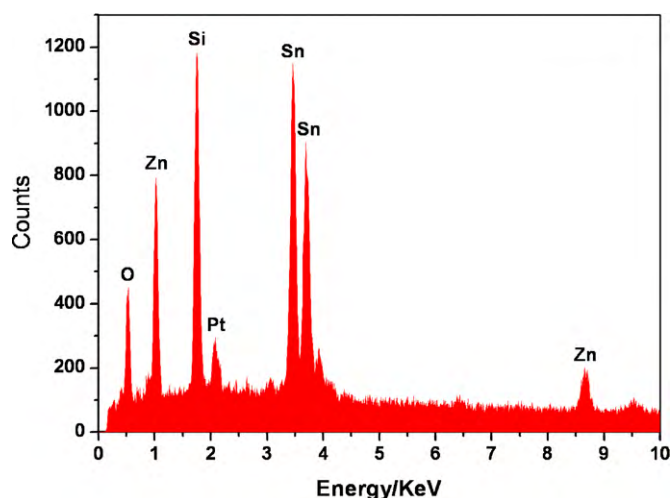


Fig. 2. EDX spectra for FTO/ZnO (0.5 M) substrate.

2.4. Photoelectrochemical and electrochemical measurements

A 500W Xenon light source (Oriol 91192, USA) was used to give an irradiance of 100 mW cm^{-2} (AM 1.5, global) which was calibrated by a Si photodiode. The current–voltage characteristics of the cells were recorded by applying external potential bias to the device and measuring the generated photocurrent with a source meter (model 2400, Keithly Instruments Inc., USA). The irradiated area of each cell was kept as 0.25 cm^2 by using a light-tight metal mask for all samples. Impedance measurements were performed with a computer-controlled electrochemical workstation (CHI660C, CH Instruments) under the bias voltage of 0.7 V in the illumination. The frequency range was 0.05–100 KHz and the magnitude of modulation signal was 0.01 V.

3. Results and discussion

3.1. Characterization of the FTO/ZnO substrate

To confirm the formation of ZnO on the FTO substrates, an EDX measurement was carried out as shown in Fig. 2. We can clearly distinguish the peak position of zinc from others, which are Sn, Si, O of which FTO is composed and Pt element resulting from vacuum deposition of Pt to increase conductivity. As shown in Fig. 2, chemical atomic wt% composition analysis for silicon, tin, zincum and oxygen elements estimated from the EDX spectrum well supported the formation of ZnO on the FTO substrates. The concentration of $\text{Zn}(\text{CH}_3\text{COO})_2$ strongly affects the thickness of ZnO film when spin-coated under the same rotate speed and time, as indicated by the relationship between thickness and $\text{Zn}(\text{CH}_3\text{COO})_2$ concentration shown in Fig. 3. It is obvious from Fig. 3 that the thickness of ZnO film goes up linearly with the increase of $\text{Zn}(\text{CH}_3\text{COO})_2$ concentration, and the blocking effect of electrons injection from TiO_2 to FTO will also be enhanced, which is discussed in Section 3.2. Fig. 4 shows the SEM surface morphology of ZnO layer on the FTO substrates. From the surface of FTO/ZnO (0.1 M) substrate we can still observe the characteristic morphology of tin oxide crystals, since the thickness of ZnO film is relatively thinner and only about 50 nm (Fig. 3). As can be seen from Fig. 4, the higher the concentration of $\text{Zn}(\text{CH}_3\text{COO})_2$, the more the surface gets flatter, and the ZnO particle grows slightly in size.

In addition, it is necessary for us to investigate the optical properties of the substrates after introducing the compact blocking film, since the devices were illuminated from FTO substrate side in working condition. Fig. 5 shows the UV–vis spectra of the bare FTO

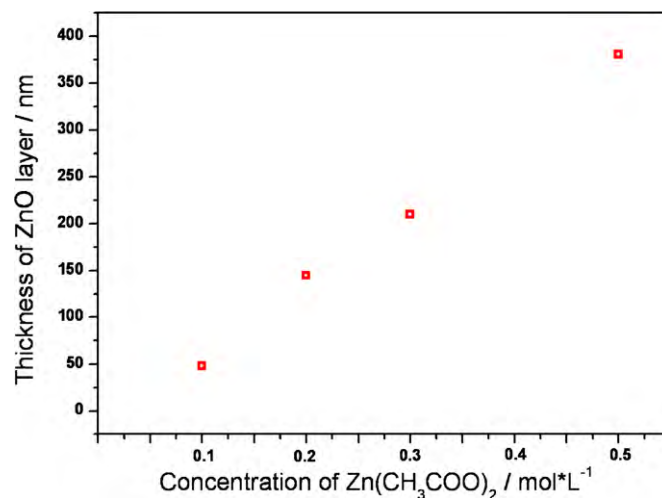


Fig. 3. The thickness of ZnO layer dependence on the concentration of zinc acetate.

and FTO/ZnO substrates. In the region from 400 nm to 800 nm, the absorption and the transmission of FTO/ZnO do not change almost compared with those of bare FTO substrate, which implies that the ZnO film will not influence the harvest of light in the most region of visible light. Though, the transmission obviously decreases (absorption increases) with the increment of $\text{Zn}(\text{CH}_3\text{COO})_2$ concentration in the region from 300 nm to 400 nm, the optical transmission of FTO/ZnO substrates in the whole region of visible light are sufficiently high to be employed in DSSCs. The slightly differences in the optical properties of the substrates with and without ZnO film may be used to explain partial electrochemical characterization of the devices, e.g. the decrease of short-circuit photocurrent density (J_{sc}).

3.2. Influence of ZnO compact blocking layer on the performance of DSSCs

Fig. 6(a) shows the photocurrent density–voltage characteristics of DSSCs based on the FTO/ZnO and bare FTO substrates at AM 1.5 irradiation of 100 mW cm^{-2} . Detailed photovoltaic performance parameters of DSSCs with different substrates are listed in Table 1. The short-circuit photocurrent density (J_{sc}), open-circuit voltage (V_{oc}) and fill factor (FF) of device without ZnO film were 16.48 mA cm^{-2} , 636.36 mV and 0.56, respectively, corresponding to an energy conversion efficiency of 5.85%. After spin-coating a ZnO film at the interface of FTO/ TiO_2 , the device gave improvement in open-circuit voltage and fill factor, while J_{sc} decreased to some extent with the increase of $\text{Zn}(\text{CH}_3\text{COO})_2$ concentration. Especially in the case of FTO/ZnO (0.2 M), the device gave an improvement of V_{oc} about 50 mV and fill factor increased by 16.1% (from 0.56 to 0.65) with J_{sc} decrease by 8.8% (from 16.48 to 15.02 mA cm^{-2}), finally resulting in the highest energy conversion efficiency 6.7% which was 14.5% higher than the device based on bare FTO substrate. It shows the merits of introducing ZnO compact blocking

Table 1

The performance of DSSCs without and with ZnO compact blocking layer^a.

Sample	J_{sc} (mA cm^{-2})	V_{oc} (mV)	FF	Eff (%)
FTO	16.48	636.36	0.56	5.85
FTO/ZnO (0.1 M) ^b	15.79	655.53	0.56	6.08
FTO/ZnO (0.2 M)	15.02	690.05	0.65	6.70
FTO/ZnO (0.3 M)	13.77	690.51	0.67	6.38
FTO/ZnO (0.5 M)	11.18	692.02	0.68	5.23

^a The parameters were tested under AM 1.5 full sunlight (100 mW cm^{-2}).

^b The numerical value in parentheses was the concentration of zinc acetate.

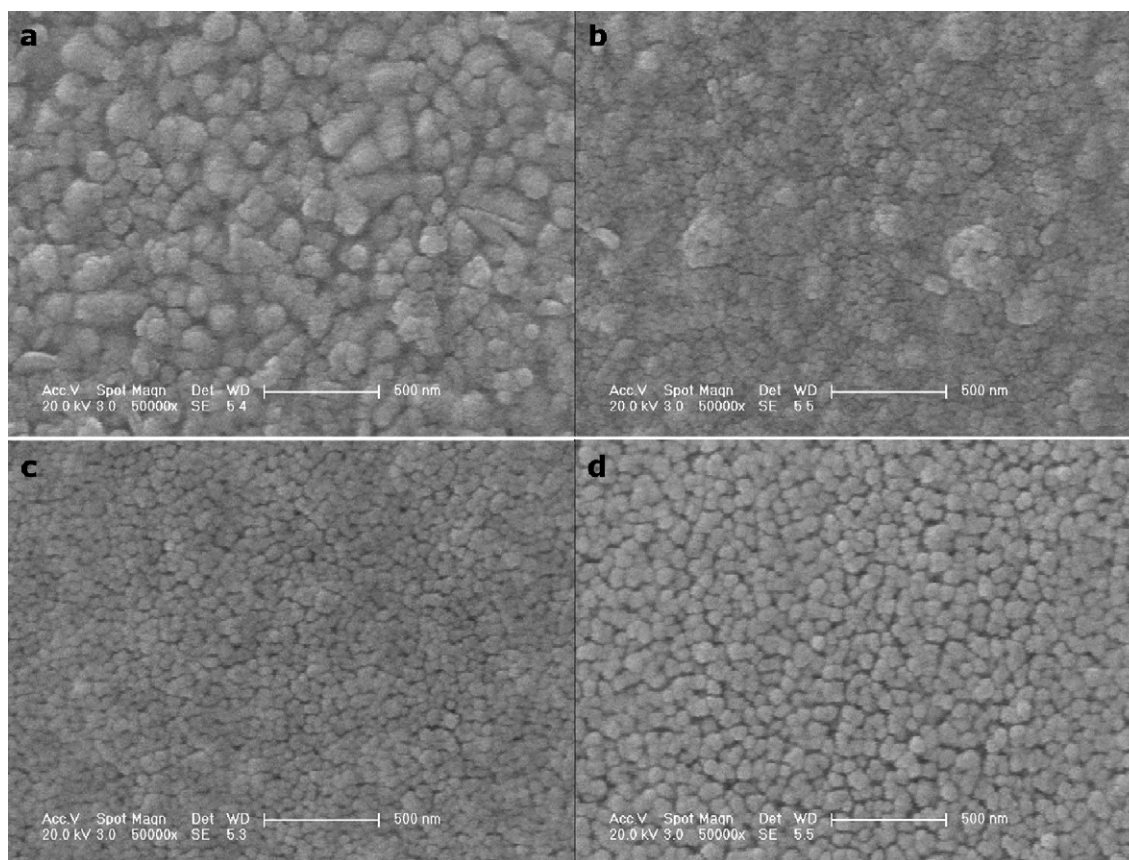


Fig. 4. Scanning electron micrograph of the surface morphology of (a) FTO and ZnO compact blocking layers with (b) 0.1 M, (c) 0.2 M, (d) 0.5 M zinc acetate concentration after calcinations at 500 °C.

film at FTO/TiO₂ interface by spin-coating method. Upon further increasing the concentration of Zn(CH₃COO)₂, V_{oc} and FF changed slightly, however, J_{sc} decreased which resulted in the reduction of energy conversion efficiency. Upon increasing the concentration of Zn(CH₃COO)₂ to 0.5 M, the ZnO compact blocking layer (360 nm, as shown in Fig. 2) became excessively thick, which resulted in the drastic decrease of J_{sc} (from 16.48 to 11.18 mA cm⁻²). This was due to the strong effect of an energy barrier by blocking the electrons injected from conductive band of TiO₂ to FTO substrate and the slightly decrease of transmission in the shortwave region (Fig. 5). Therefore, it is very important to control and optimize the thickness of ZnO layer by adjusting the concentration of Zn(CH₃COO)₂.

To investigate the effect of ZnO film of suppressing back electrons transfer from FTO to electrolytes, the photocurrent density-voltage characteristics were also measured in the dark. As can be seen in Fig. 6(b), the dark current of DSSCs based on FTO/ZnO substrates decreased markedly compared with bare FTO. And the dark current decreased with the increase of Zn(CH₃COO)₂ concentration. The reduction of the dark current demonstrates that the ZnO layers successfully reduced the reaction sites for the charge recombination between electrons emanating from the FTO substrate and I₃⁻ ions present in the electrolyte [27], and implies that ZnO is a good material for the compact layer in DSSCs. Meanwhile, the effect of ZnO film of suppressing the dark current will relax the blocking effect for electrons injection, which probably reduces the decay of J_{sc} .

Electrochemical impedance spectroscopy (EIS) analysis has been regarded as a useful tool for investigating the electron-transport and recombination in DSSCs. To further characterize the kinetics of electrochemical progress occurring in DSSCs based on FTO/ZnO substrate and the effect of ZnO layer, the electrochemical

impedance spectroscopy of DSSCs based on FTO and FTO/ZnO substrates were measured in the illumination with the bias voltage of 0.7 V. Fig. 7 shows Nyquist plots of DSSCs based on FTO, FTO/ZnO (0.2 M), FTO/ZnO (0.5 M) substrates. The impedance components of the interfaces in DSSCs observed in the frequency regions of 10³ to 10⁵ Hz (ω_1), 1 to 10³ Hz (ω_2), 0.1 to 1 Hz (ω_3) are associated with the charge transport at the FTO/TiO₂ and Pt counter electrode/electrolyte interfaces (Z_1), the TiO₂/dye/electrolyte interfaces (Z_2), and the Nernstian diffusion in the electrolyte (Z_3), respectively [28,29]. Table 2 summarized the results of EIS analysis fitted by using an equivalent circuit containing a constant phase element (CPE) and resistance (R) (Fig. 7, inset). The resistance of the Z_1 component (R_1), which is given by the sum of resistances of counter electrode/electrolyte and FTO/TiO₂ interfaces [30], increased to some extent upon spin-coating ZnO film. Since an identical Pt counter electrode was employed for all the devices, the noticeable difference at the interfaces of FTO/TiO₂ was wholly responsible for the increase of R_1 . R_1 of DSSCs based on bare FTO substrate (4.14 Ω) was lower to that of FTO/ZnO (0.2 M) (4.80 Ω), and the sample of FTO/ZnO (0.5 M) achieved the highest R_1 resistance (14.98 Ω). This implies that the existence of ZnO layer increased the interfacial resistance between FTO substrate and TiO₂, since the conduction band edge of ZnO is more negative than that of TiO₂, which resulted in the form of an energy bar-

Table 2
Fitting results of EIS analysis.

Sample	R_1 (Ω)	R_2 (Ω)	ω_{max} of Z_2 (Hz)
FTO	4.14	20.84	4.54
FTO/ZnO (0.2 M)	4.80	16.29	6.64
FTO/ZnO (0.5 M)	14.98	15.42	11.91

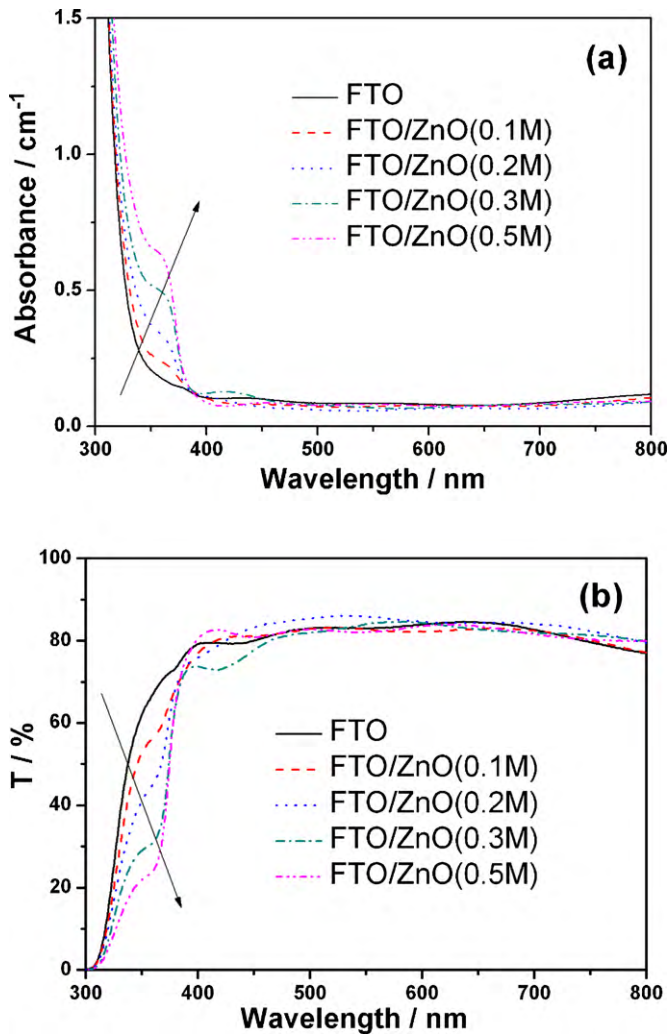


Fig. 5. Optical properties of bare FTO and FTO/ZnO substrates with different concentration of zinc acetate. (a) absorption spectra (b) transmission spectra.

rier at the interface of FTO/TiO₂. This energy barrier will block the electrons injected from the conductive band of TiO₂ to FTO, so the short-circuit photocurrent density (J_{sc}) of DSSCs based on FTO/ZnO substrates decreased compared to that of bare FTO, which was in good agreement with the previous photocurrent density-voltage characteristics. As a consequence, the photogenerated electrons will accumulate in the conductive band of TiO₂, which led to the increment of electron density in TiO₂, and thus the shift of Fermi level for electrons in the TiO₂ electrode. In general, the open-circuit voltage (V_{oc}) value of a DSSC is defined as the difference in energy between Fermi level of the photoelectrode semiconductor oxide and the redox potential of the electrolyte [31,32]. Therefore, the rise of Fermi level resulting from the increase of electron density in the conductive band of TiO₂ will improve the V_{oc} remarkably, which has been demonstrated by the photocurrent density-voltage characteristics. In addition, R_2 , the resistance of interfacial charge-transfer from the TiO₂ to triiodide in the electrolyte, decreases due to the increase of electron density in the TiO₂ [33,34]. As shown in Table 2, R_2 of DSSCs based on bare FTO, FTO/ZnO (0.2 M) and FTO/ZnO (0.5 M) substrates were 20.84 Ω , 16.29 Ω and 15.42 Ω , respectively, which also demonstrated the increase of electron density in the conductive band of TiO₂ after introducing the ZnO as the compact blocking layer. On the other hand, the electron lifetime in TiO₂ is inversely proportional to the frequency of maximum Z'' at

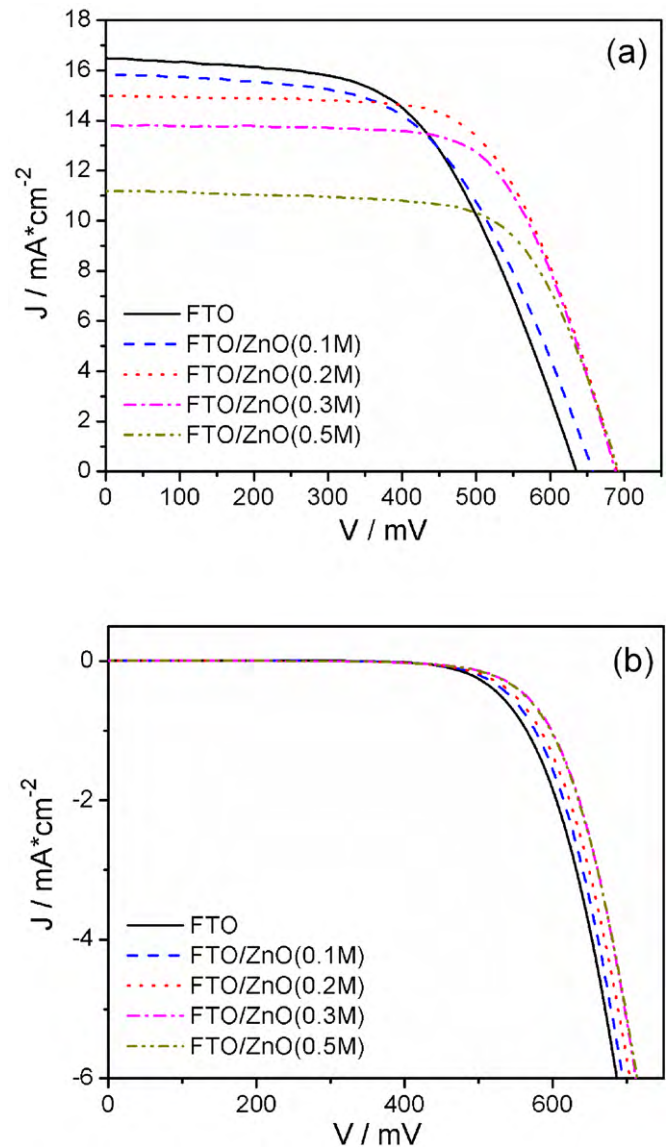


Fig. 6. Photocurrent density-voltage characteristics of DSSCs based on ZnO compact blocking layers with different concentration of zinc acetate: (a) measured under AM 1.5 irradiation of 100 mW cm⁻², (b) measured in the dark.

the Z_2 component (ω_{max}) [35].

$$\tau = \frac{1}{\omega_{max}} \quad (1)$$

As can be seen in Table 2, ω_{max} of the samples based on bare FTO, FTO/ZnO (0.2 M) and FTO/ZnO (0.5 M) substrates were 4.54 Hz, 6.64 Hz and 11.91 Hz, respectively, which increased after employing the ZnO compact blocking layer. Therefore, the electron lifetime was reduced in the present of ZnO compact blocking film, which was seldom reported in previous researches on TiO₂-based compact film.

In order to explore the origin of the decrease in electron lifetime, open-circuit voltage decay (OCVD) characteristics of devices based on bare FTO, FTO/ZnO (0.2 M) and FTO/ZnO (0.5 M) substrates were measured (Fig. 8). OCVD is a technique which monitors the subsequent decay of photovoltage (V_{oc}) after turning off the illumination in a steady state [36]. As shown in Fig. 8, it is obvious that the values of photovoltage response of the DSSCs based on FTO/ZnO substrates were higher than the device based on bare FTO in the whole time domain. It also demonstrates the increment of electron

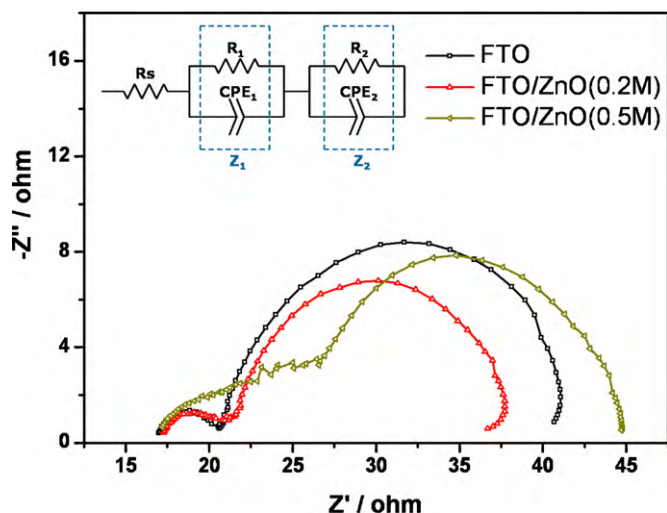


Fig. 7. Nyquist plots of DSSCs based on FTO, FTO/ZnO (0.2 M), FTO/ZnO (0.5 M) substrates. The impedance spectra were measured in the illumination with the bias voltage of 0.7 V.

density in the TiO_2 , since the decay of photovoltage reflects the decrease of the electron density in the TiO_2 , which is mainly caused by the charge recombination [37]. In other words, the recombination rate of photoelectron is proportional to the rate of photovoltage decay. Therefore, we calculated the rate of open-circuit voltage decay ($dV_{oc} \times dt^{-1}$) based on the different substrates obtained from the data shown in Fig. 8 (except the platform), which is inversely proportional to the electron lifetime as reported by others [24,25].

$$\tau = -\frac{k_B T}{e} \left(\frac{dV_{oc}}{dt} \right)^{-1} \quad (2)$$

One should pay close attention to the start point of the curve in Fig. 9, which shows the dependence of $dV_{oc} \times dt^{-1}$ on time, since the onset for the curve mainly reflects the recombination rate of photoelectron of the device in illumination corresponding to a high electron density. In the short time region, we can see that the absolute values of $dV_{oc} \times dt^{-1}$ based on FTO/ZnO were upper to bare FTO substrate, which implies that the recombination rate of photoelectron in the present of ZnO compact blocking film was higher than bare FTO substrate. Since the mesoporous TiO_2 films were prepared by the identical fabrication procedures, the density of

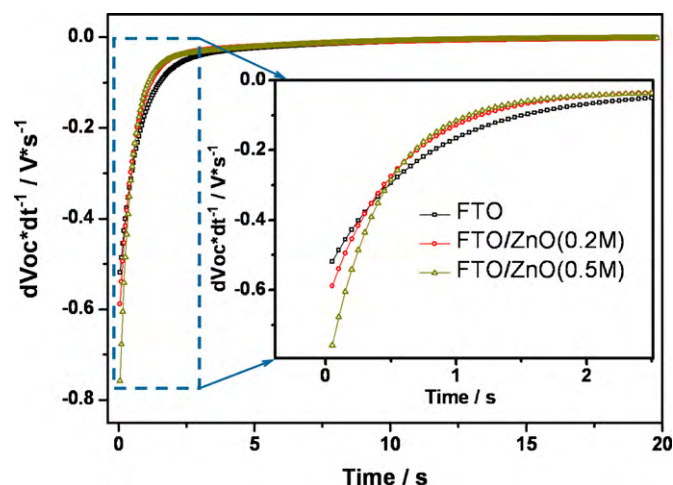


Fig. 9. Dependence of the rate of open-circuit voltage decay ($dV_{oc} \times dt^{-1}$) on time based on different substrates: FTO, FTO/ZnO (0.2 M), FTO/ZnO (0.5 M).

recombination center and bulk traps inside the TiO_2 electrode for each sample was the same. Consequently, the increase of recombination rate was mainly related to the increase of electron density after introducing the ZnO layer, resulting in the decrease of electron lifetime by Eq. (2), which was in good agreement with the value of electron lifetime (τ) corresponding to the onset of each curve in Fig. 10. In addition, the absolute value of $dV_{oc} \times dt^{-1}$ of the samples based on FTO/ZnO substrates were lower than the value of bare FTO after 0.5 s, which means that the recombination rate reduced after the electron density of the samples based on FTO/ZnO substrates decayed to a normal level, corresponding to a longer electron lifetime (τ) as shown in Fig. 10, for the main reason of suppressing back electron transfer from FTO to electrolyte.

The fill factor is a measure which reflects the increase in recombination or decrease in photocurrent with increasing photovoltage [38]. If the electron transfer rate from TiO_2 to the triiodide increases, the potential of the TiO_2 will become less negative for the decrease of the electron density in the conductive band of TiO_2 , which results in the low fill factor. Based on the foregoing discussion, one can infer that the recombination rate of photoelectron increased after introducing ZnO as the compact blocking film, however, we obtained a remarkable increment of the electron density in TiO_2 , which leads

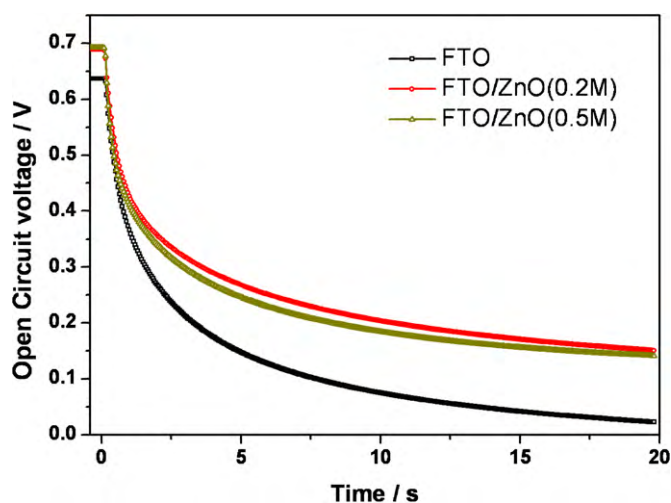


Fig. 8. Open-circuit potential decay for the DSSCs based on FTO, FTO/ZnO (0.2 M) and FTO/ZnO (0.5 M) substrates.

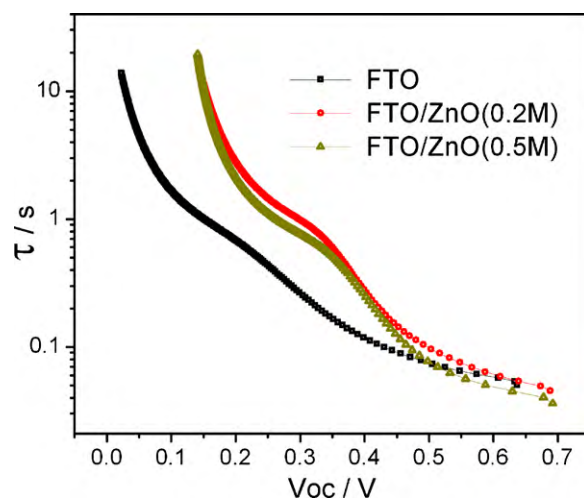


Fig. 10. Electron lifetime (in log-linear representation) as a function of open-circuit voltage (V_{oc}) for DSSCs based on different substrates: FTO, FTO/ZnO (0.2 M), FTO/ZnO (0.5 M).

that the potential of TiO₂ becomes more negative, and so the higher fill factor.

4. Conclusion

In summary, we demonstrated a methodology of introducing ZnO as a novel compact blocking film by a simple route, which created an energy barrier between the FTO substrate and mesoporous TiO₂ film, resulting in remarkable increment of electron density in the TiO₂, and greatly enhancing V_{oc} and FF. When the concentration of Zn(CH₃COO)₂ was 0.2 M corresponding to a ZnO film of thickness about 150 nm, we achieved the highest energy conversion efficiency. With the increase of Zn(CH₃COO)₂ concentration, V_{oc} and FF change slightly, however, J_{sc} decrease drastically, because the thicker ZnO film not only increased the electron density but also strongly blocked the electrons injected from the conductive band of TiO₂ to FTO substrate, which led to a lower conversion efficiency. These results were confirmed by the EIS analysis and OCVD technique. Therefore, our findings open the way for employing new materials as the compact layer in DSSCs. And further research is underway in our group to investigate the modification in the energy band structure of the compact blocking layer.

Acknowledgements

We acknowledge the financial support of the Ministry of Science and Technology of China through Hi-Tech Plan (funding no. 2006AA03Z347), and this work was partially supported by National Basic Research Program (No. 2011CB933300) of China, National Nature Science Foundation of China (50125309), National Science Fund for Talent Training in Basic Science (Grant No. J0830310) and the PhD Research Foundation of Wuhan University (20102020201000016). We also acknowledge the help of the Nanoscience and Nanotechnology Center at Wuhan University for the SEM and UV–vis spectrophotometer characterization.

References

- [1] B. O'Regan, M. Gratzel, *Nature* 353 (1991) 737.
- [2] A. Zaban, S.G. Chen, S. Chappel, B.A. Gregg, *Chem. Commun.* 22 (2000) 2231.
- [3] S.J. Wu, H.W. Han, Q.D. Tai, J. Zhang, B.L. Chen, S. Xu, C.H. Zhou, Y. Yang, H. Hu, X.Z. Zhao, *Appl. Phys. Lett.* 92 (2008) 122106.
- [4] S.S. Kim, J.H. Yum, Y.E. Sung, *J. Photochem. Photobiol. A* 171 (3) (2005) 269.
- [5] S.J. Wu, H.W. Han, Q.D. Tai, J. Zhang, S. Xu, C.H. Zhou, Y. Yang, H. Hu, B.L. Chen, B. Sebo, X.Z. Zhao, *Nanotechnology* 19 (2008) 215704.
- [6] T. Taguchi, X.T. Zhang, I. Sutanto, K. Tokuhira, T.N. Rao, H. Watanabe, T. Nakamori, M. Uragami, A. Fujishima, *Chem. Commun.* 19 (2003) 2480.
- [7] S.J. Wu, H.W. Han, Q.D. Tai, J. Zhang, S. Xu, C.H. Zhou, Y. Yang, H. Hu, B.L. Chen, X.Z. Zhao, *J. Power Sources* 182 (1) (2008) 119.
- [8] E. Palomares, J.N. Clifford, S.A. Haque, T. Lutz, J.R. Durrant, *J. Am. Chem. Soc.* 125 (2) (2003) 475.
- [9] Y. Diamant, S.G. Chen, O. Melamed, A. Zaban, *J. Phys. Chem. B* 107 (9) (2003) 1977.
- [10] S.M. Yang, Y.Y. Huang, C.H. Huang, X.S. Zhao, *Chem. Mater.* 14 (4) (2002) 1500.
- [11] S.A. Haque, T. Park, C. Xu, S. Koops, N. Schulte, R.J. Potter, A.B. Holmes, J.R. Durrant, *Adv. Funct. Mater.* 14 (5) (2004) 435.
- [12] B.A. Gregg, F. Pichot, S. Ferrere, C.L. Fields, *J. Phys. Chem. B* 105 (7) (2001) 1422.
- [13] B. Peng, G. Jungmann, C. Jager, D. Haarer, H.W. Schmidt, M. Thelakkat, *Coord. Chem. Rev.* 248 (13–14) (2004) 1479.
- [14] S. Hore, R. Kern, *Appl. Phys. Lett.* 87 (2005) 263504.
- [15] K. Zhu, E.A. Schiff, N.G. Park, J. van de Lagemaat, A. Frank, *J. Appl. Phys. Lett.* 80 (4) (2002) 685.
- [16] H. Yu, S.Q. Zhang, H.J. Zhao, G. Will, P.R. Liu, *Electrochim. Acta* 54 (4) (2009) 1319.
- [17] A.O.T. Patrocinio, L.G. Paterno, N.Y.M. Iha, *J. Photochem. Photobiol. A* 205 (1) (2009) 23.
- [18] S. Ito, T.N. Murakami, P. Comte, P. Liska, C. Gratzel, M.K. Nazeeruddin, M. Gratzel, *Thin Solid Films* 516 (14) (2008) 4613.
- [19] J.B. Xia, N. Masaki, K.J. Jiang, S. Yanagida, *Chem. Commun.* 2 (2007) 138.
- [20] J.B. Xia, N. Masaki, K.J. Jiang, S. Yanagida, *J. Phys. Chem. C* 111 (22) (2007) 8092.
- [21] S. Lee, J.H. Noh, H.S. Han, D.K. Yim, D.H. Kim, J.K. Lee, J.Y. Kim, H.S. Jung, K.S. Hong, *J. Phys. Chem. C* 113 (16) (2009) 6878.
- [22] J.H. Noh, S. Lee, J.Y. Kim, J.K. Lee, H.S. Han, C.M. Cho, I.S. Cho, H.S. Jung, K.S. Hong, *J. Phys. Chem. C* 113 (3) (2009) 1083.
- [23] S.J. Roh, R.S. Mane, S.K. Min, W. Lee, *J. Appl. Phys. Lett.* 89 (2006) 253512.
- [24] H. Horiuchi, R. Katoh, K. Hara, M. Yanagida, S. Murata, H. Arakawa, M. Tachiya, *J. Phys. Chem. B* 107 (11) (2003) 2570.
- [25] M.F. Hossain, S. Biswas, M. Shahjahan, T. Takahashi, *J. Vac. Sci. Technol. A* 27 (4) (2009) 1047.
- [26] R.L. Willis, C. Olson, B. O'Regan, T. Lutz, J. Nelson, J.R. Durrant, *J. Phys. Chem. B* 106 (31) (2002) 7605.
- [27] S. Ito, P. Liska, P. Comte, R.L. Charvet, P. Pechy, U. Bach, L. Schmidt-Mende, S.M. Zakeeruddin, A. Kay, M.K. Nazeeruddin, M. Gratzel, *Chem. Commun.* 34 (2005) 4351.
- [28] R. Kern, R. Sastrawan, J. Ferber, R. Stangl, J. Luther, *Electrochim. Acta* 47 (26) (2002) 4213.
- [29] L.Y. Han, N. Koide, Y. Chiba, T. Mitate, *Appl. Phys. Lett.* 84 (13) (2004) 2433.
- [30] T. Hoshikawa, R. Kikuchi, K. Eguchi, *J. Electroanal. Chem.* 588 (1) (2006) 59.
- [31] J. Van de Lagemaat, N.G. Park, A.J. Frank, *J. Phys. Chem. B* 104 (9) (2000) 2044.
- [32] S. Burnside, J.E. Moser, K. Brooks, M. Gratzel, D. Cahen, *J. Phys. Chem. B* 103 (43) (1999) 9328.
- [33] F. Fabregat-Santiago, J. Bisquert, G. Garcia-Belmonte, G. Boschloo, A. Hagfeldt, *Sol. Energ. Mater. Sol. C* 87 (1–4) (2005) 117.
- [34] F. Fabregat-Santiago, J. Bisquert, E. Palomares, L. Otero, D.B. Kuang, S.M. Zakeeruddin, M. Gratzel, *J. Phys. Chem. C* 111 (17) (2007) 6550.
- [35] M. Adachi, M. Sakamoto, J.T. Jiu, Y. Ogata, S. Isoda, *J. Phys. Chem. B* 110 (28) (2006) 13872.
- [36] J. Bisquert, A. Zaban, M. Greenshtein, I. Mora-Sero, *J. Am. Chem. Soc.* 126 (41) (2004) 13550.
- [37] A. Zaban, M. Greenshtein, J. Bisquert, *Chemphyschem* 4 (8) (2003) 859.
- [38] D. Cahen, G. Hodes, M. Gratzel, J.F. Guillemoles, I. Riess, *J. Phys. Chem. B* 104 (9) (2000) 2053.